Cell Metabolism
Article

Cholesterol-Dependent Degradation of Squalene Monooxygenase, a Control Point in Cholesterol Synthesis beyond HMG-CoA Reductase

Saloni Gill,[1,2] Julian Stevenson,[1,2] Ika Kristiana,[1] and Andrew J. Brown[1,*]
[1]School of Biotechnology and Biomolecular Sciences, University of New South Wales, Sydney NSW 2052, Australia
[2]These authors contributed equally to this work
*Correspondence: aj.brown@unsw.edu.au
DOI 10.1016/j.cmet.2011.01.015

SUMMARY

Exquisite control of cholesterol synthesis is crucial for maintaining homeostasis of this vital yet potentially toxic lipid. Squalene monooxygenase (SM) catalyzes the first oxygenation step in cholesterol synthesis, acting on squalene before cyclization into the basic steroid structure. Using model cell systems, we found that cholesterol caused the accumulation of the substrate squalene, suggesting that SM may serve as a flux-controlling enzyme beyond 3-hydroxy-3-methylglutaryl-coenzyme A reductase (HMGR, considered as rate limiting). Cholesterol accelerated the proteasomal degradation of SM which required the N-terminal domain, partially conserved in vertebrates but not in lower organisms. Unlike HMGR, SM degradation is not mediated by Insig, 24,25-dihydrolanosterol, or side-chain oxysterols, but rather by cholesterol itself. Importantly, SM's N-terminal domain conferred cholesterol-regulated turnover on heterologous fusion proteins. Furthermore, proteasomal inhibition almost totally eliminated squalene accumulation, highlighting the importance of this degradation mechanism for the control of SM and suggesting this as a possible control point in cholesterol synthesis.

INTRODUCTION

Cholesterol is a vital lipid in animals, but also can be toxic in excess. Consequently, elaborate homeostatic mechanisms have evolved, with exquisite control of cholesterol levels occurring at multiple levels within the cell (Goldstein et al., 2006). Research into the regulation of cholesterol synthesis has centered on 3-hydroxy-3-methylglutaryl-coenzyme A reductase (HMGR). It catalyzes a major "rate-limiting" step or control point in cholesterol synthesis (Rodwell et al., 1976), yielding mevalonate, and is the target of the statin class of drugs used to treat hypercholesterolemia. HMGR is regulated by several mechanisms, notably by the transcription factor SREBP-2 (sterol regulatory element binding protein-2), and through proteasomal degradation via Insig binding to its sterol-sensing domain (DeBose-Boyd, 2008). In contrast, relatively little is known about the regulatory role and control of other enzymes in the pathway, although most are known SREBP-2 target genes (Horton et al., 2003).

One such enzyme is squalene monooxygenase (SM), formerly squalene epoxidase (EC 1.14.99.7). SM is a microsomal flavin monooxygenase (Yamamoto and Bloch, 1970) that catalyzes the first oxygenation step in cholesterol synthesis, the conversion of squalene to the nonsterol precursor for lanosterol, 2,3 (*S*)-monooxidosqualene (MOS) (Figure S1A available online). SM is important clinically as the target of fungicides such as terbinafine (Chugh et al., 2003). In addition, a number of natural compounds proposed to reduce serum cholesterol levels in humans inhibit this enzyme, such as polyphenols in green tea, resveratrol in wine, and garlic extract (Abe et al., 2000; Gupta and Porter, 2001). Although not widely appreciated, SM has been proposed to be a second rate-limiting enzyme in cholesterol synthesis (Gonzalez et al., 1979; Hidaka et al., 1990). The precursor squalene accumulates when Chinese hamster ovary (CHO) cells (Eilenberg and Shechter, 1984), human fibroblasts (Brown and Goldstein, 1980), rat hepatoma cells, and renal carcinoma cells (Gonzalez et al., 1979) are incubated with radiolabeled mevalonate and exogenous sterols. Similar accumulation has also been observed using rat and dog kidney slices (Raskin and Siperstein, 1974). Furthermore, the concept that SM may be a largely overlooked control point in cholesterol synthesis is suggested by its much lower specific activity in liver cells compared to that of HMGR (Hidaka et al., 1990).

As an SREBP-2 target, SM expression is modulated by sterols, increasing under lipid-depleted conditions (Hidaka et al., 1990; Nagai et al., 2002). Here, we report that SM is also posttranslationally regulated by cholesterol-dependent proteasomal degradation. Inhibition of the proteasome prevents squalene accumulation in response to cholesterol treatment, suggesting that this mechanism constitutes a possible control point in cholesterol synthesis beyond HMGR.

RESULTS

Cholesterol Treatment Causes Squalene to Accumulate

A key observation that highlights the rate-limiting activity of SM is squalene accumulation when cholesterol levels are high (Brown and Goldstein, 1980; Eilenberg and Shechter, 1984; Gonzalez et al., 1979). These experiments were conducted

with radiolabeled mevalonate, consequently bypassing HMGR. We labeled CHO-7 cells for 4 hr with [^{14}C]-acetate, which feeds into the beginning of the cholesterol biosynthetic pathway. CHO-7 cells were chosen because they can be maintained in lipoprotein-deficient serum (LPDS) (Metherall et al., 1989), which offers considerable flexibility in manipulating cholesterol levels. Importantly, we found that treatment of CHO-7 cells with sterols and [^{14}C]-acetate also led to the accumulation of [^{14}C]-squalene (Figure 1A). This band was absent upon inhibition of squalene synthase (lane 1) and accumulated when SM was inhibited (lane 2). The most striking squalene accumulation resulted from addition of cholesterol complexed with methyl-β-cyclodextrin (Chol/CD, lane 5), followed by low-density lipoprotein (LDL) (lane 4), and then the oxysterol 25-hydroxycholesterol (25HC) (lane 6). Thus, in this system, cholesterol treatment induces squalene accumulation, raising the possibility of a rate-limiting step after HMGR involving SM.

Experiments examining cholesterol homeostasis commonly use statin pretreatment, which reduces cellular cholesterol status and increases the expression of cholesterogenic genes (Wong et al., 2008). Under these conditions, HMGR activity may be increased sufficiently such that it is no longer rate-limiting, producing a bottleneck downstream at SM. To address this possibility, acute cholesterol treatment (Chol/CD and LDL) was repeated for CHO-7 cells maintained in full serum without statin pretreatment (Figure 1B). Squalene accumulated markedly when cells were grown in full serum (lane 4), albeit to a lesser extent than seen for LPDS (lane 2). Squalene accumulation was also observed with or without the statin pretreatment (Figure S1B), that is, whether or not HMGR was first inhibited. Furthermore, if cholesterol treatment were to inactivate HMGR faster than SM, then accumulation of squalene (occurring after HMGR) would not be observed. Thus, cholesterol treatment caused squalene to accumulate under a variety of culturing conditions, suggesting that altered activity of earlier enzymes in the pathway, such as HMGR, is insufficient to explain the squalene accumulation. Furthermore, the effect is not restricted to CHO-7 cells (Figure 1C): a cholesterol-dependent increase in squalene accumulation was also seen in three human cell-lines of hepatic (HepG2), neuronal [BE(2)C], and renal (HEK293) origin, as well as in primary human fibroblasts (Fb).

When examined over time, cholesterol treatment led to the progressive accumulation of squalene and decreased de novo cholesterol synthesis (Figure 1D), most notably after 4 hr (lane 5), but also as early as 2 hr (lane 3). In the absence of exogenous cholesterol, the levels of newly synthesized cholesterol were relatively constant, with no observed squalene. These results suggest that SM becomes rate-limiting due to an acute cholesterol-dependent regulatory mechanism.

To uncover this mechanism, we first examined transcriptional regulation using quantitative (real-time) PCR and compared the messenger RNA (mRNA) levels of *SQLE* (SM) to that of *HMGCR* (HMGR). In the absence of added cholesterol, the mRNA levels of both genes were constant and remained unaffected over 16 hr (Figure 1E). The addition of cholesterol caused a decrease in expression levels of both genes with similar kinetics and magnitude. Therefore, there is dissociation of mRNA levels from flux through the pathway, suggesting posttranscriptional regulation of SM.

Cholesterol-Dependent Posttranscriptional Regulation of SM

To exclude transcriptional regulation, we utilized SRD-1 cells, a mutant line of CHO cells which exhibit sterol-independent expression of SREBP-2 target genes (Yang et al., 1994). These cells overexpress a truncated form of SREBP-2, bypassing the sterol-regulated proteolytic step, leading to constant transcriptional activation regardless of sterol levels. Thus, mRNA levels of *HMGCR* and *SQLE* were similarly unaffected by cholesterol addition (Figure 2A). Nevertheless, cholesterol-dependent squalene accumulation was still evident in SRD-1 cells (Figure 2B). This is consistent with SM being posttranscriptionally regulated by cholesterol, which may impact on the control of cholesterol synthesis.

Cholesterol-Dependent Degradation of SM

One explanation for the accumulation of squalene is that cholesterol also acts posttranslationally, accelerating the degradation of SM. We investigated this possibility in SRD-1 cells (Figure 3A). Chol/CD caused a reduction in endogenous SM protein from 4 hr, with negligible levels by 8 hr (lane 7). This effect was not observed when cells were treated with methyl-β-cyclodextrin (CD) without cholesterol (Figure 3B, lane 3). Protein synthesis was inhibited with cycloheximide (CHX) during cholesterol treatment, showing that the regulation was posttranslational, through degradation of SM. This cholesterol-mediated degradation of SM was on a comparably acute timescale to squalene accumulation (cf. Figure 2B). Overall, addition of cholesterol increased SM turnover several-fold, with the estimated half-life decreasing from ~14 hr to ~4 hr. Exogenous cholesterol derived solely from serum also appeared to promote degradation (Figure S2): SM protein levels were lower in full serum (NCS) compared with cholesterol-depleted serum (LPDS) after 8 hr.

Sterol Specificity—Cholesterol as the Principal Degradative Signal

Next, we examined whether endogenously synthesized sterols could regulate SM. We pretreated cells for 16 hr with a statin to inhibit sterol synthesis, lowering cholesterol levels and upregulating SREBP-2 target genes. The removal of the statin from the media then allows increased sterol synthesis due to the higher level of biosynthetic enzymes (Wong et al., 2008). Total cellular cholesterol at 8 hr increased by ~20% when statin was withdrawn from SRD-1 cells (an increase of 7 μg/mg from 34 μg/mg cell protein). This newly synthesized sterol was sufficient to accelerate the degradation of SM (Figure 4A). Inhibiting later steps in the mevalonate pathway, at SM and lanosterol synthase (the first sterol generating enzyme), preserved SM protein levels to the same extent as statin (Figure 4B, lanes 1, 3, and 5), indicating that the degradative signal is a sterol.

To examine the sterol specificity of this potential regulatory mechanism, we tested the ability of a selection of sterol pathway intermediates and oxysterols to cause degradation of ectopic, human SM. Consistent with our results for endogenous hamster protein, there was a cholesterol-dependent reduction in human SM (with expression in CHO-7 cells driven by a thymidine kinase [TK] promoter) (Figure 4C, lanes 3 and 4). In contrast, a construct with a higher expression cytomegalovirus (CMV) promoter did not show clear sterol regulation (lanes 7 and 8).

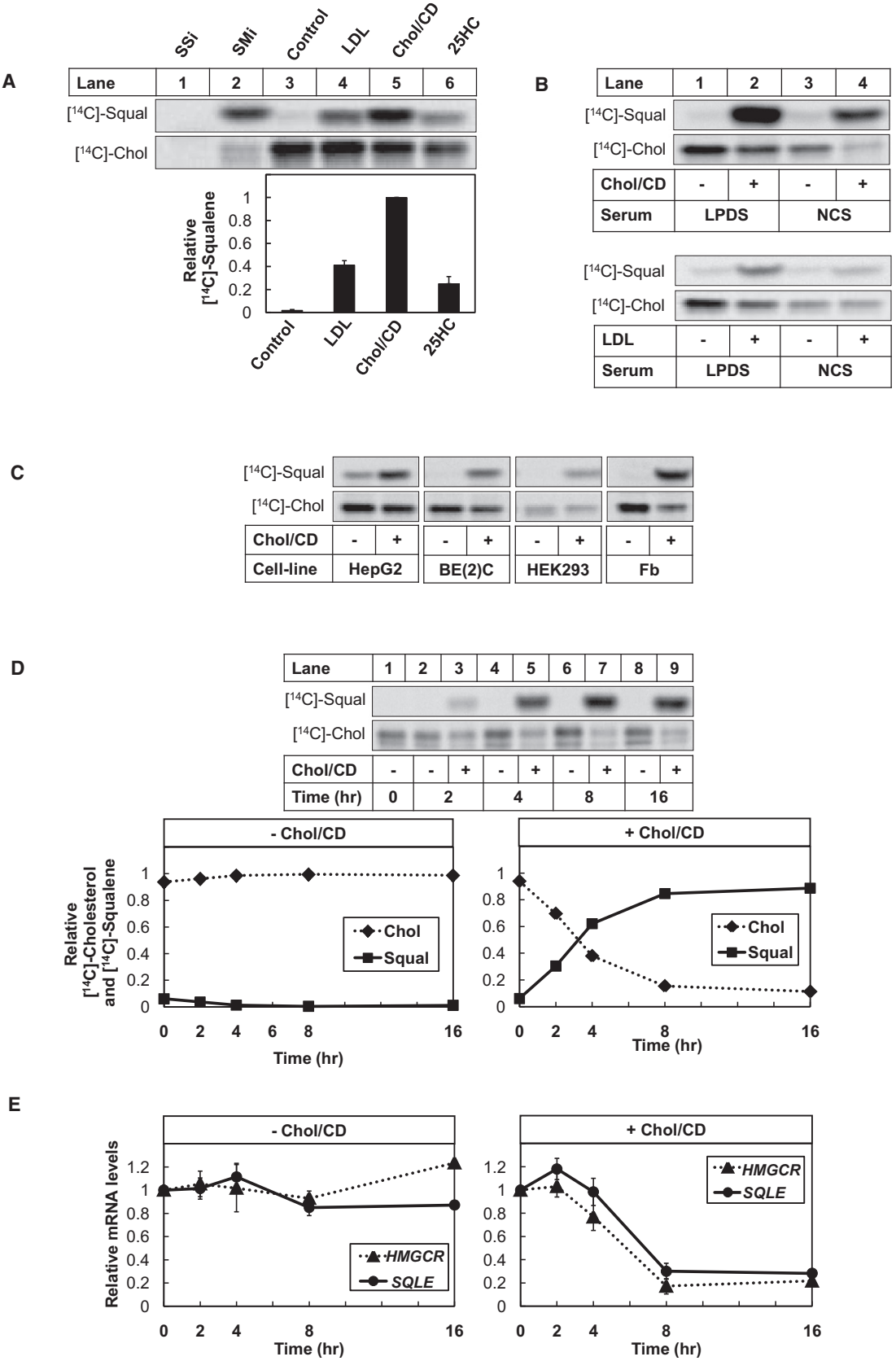
A
SSi
SMi
Control
LDL
Chol/CD
25HC
Lane 1 2 3 4 5 6
[14C]-Squal
[14C]-Chol
Relative [14C]-Squalene
Control
LDL
Chol/CD
25HC
B
Lane 1 2 3 4
[14C]-Squal
[14C]-Chol
Chol/CD - + - +
Serum LPDS NCS
[14C]-Squal
[14C]-Chol
LDL - + - +
Serum LPDS NCS
C
[14C]-Squal
[14C]-Chol
Chol/CD - + - + - + - +
Cell-line HepG2 BE(2)C HEK293 Fb
D
Lane 1 2 3 4 5 6 7 8 9
[14C]-Squal
[14C]-Chol
Chol/CD - - + - + - + - +
Time (hr) 0 2 4 8 16
- Chol/CD
+ Chol/CD
Relative [14C]-Cholesterol and [14C]-Squalene
Chol
Squal
Time (hr)
E
- Chol/CD
+ Chol/CD
Relative mRNA levels
HMGCR
SQLE
Time (hr)

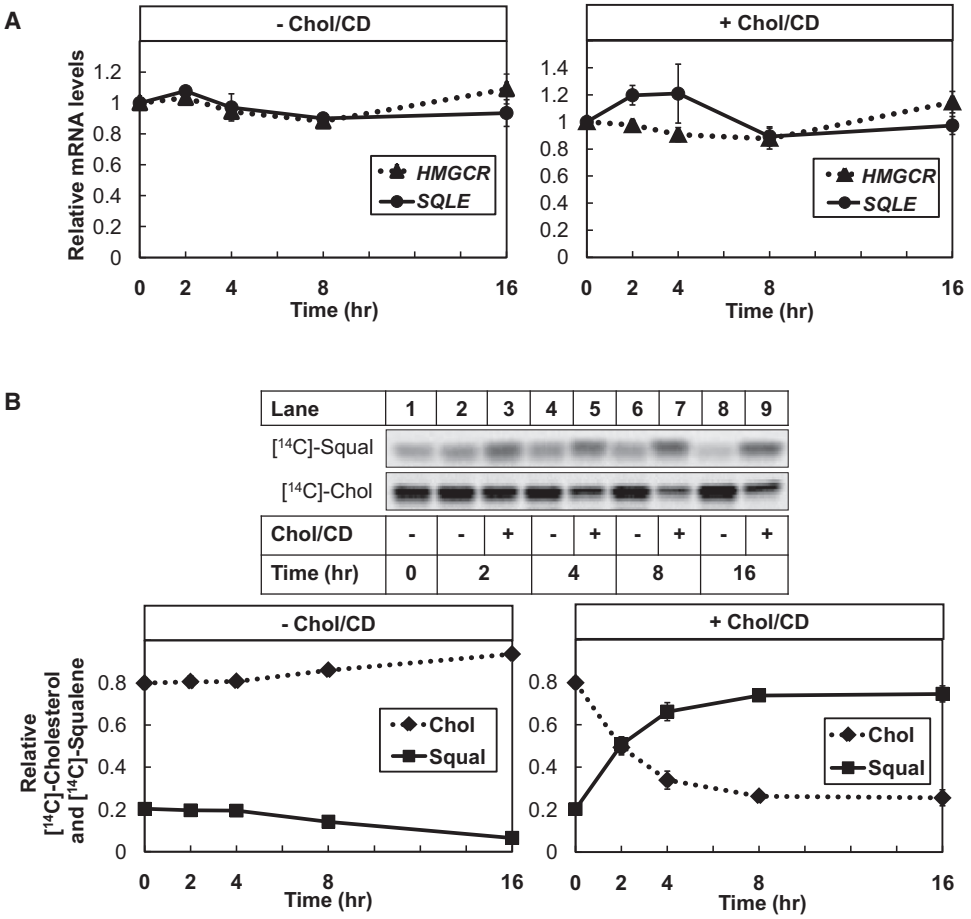

Figure 2. Cholesterol Treatment Causes Squalene to Accumulate in SRD-1 Cells, Independent of Transcriptional Regulation

(A) Cells were treated as in Figure 1E (n = 3, each performed in triplicate, ± SEM).

(B) Cells were treated and data presented as in Figure 1D (n = 4, ± SEM).

The TK construct was used to test oxysterols, which have one or more additional oxygen-containing groups on the carbon backbone of cholesterol or related sterols (Figure 4D). A concentration of 25HC (1 μg/ml) commonly used to inhibit SREBP processing (Adams et al., 2004) did not destabilize SM, nor did 24,25EC (1 μg/ml), a physiological regulator of cholesterol synthesis (Wong et al., 2008) (Figure 4E). A range of sterols and oxysterols were delivered complexed in methyl-β-cyclodextrin at the same concentration as cholesterol (20 μg/ml; Figures 4F and 4G). Treatment with the side-chain oxysterols 24,25EC, 25HC, and 27-hydroxycholesterol (27HC) again had no effect on SM protein levels (Figure 4F, lanes 6–8), in contrast to what

Figure 1. Cholesterol Treatment Causes Squalene to Accumulate in Various Cells

(A, C, and D) Cells were statin pretreated overnight, treated with test agents as indicated, labeled with [^{14}C]-acetate, and assayed for [^{14}C]-cholesterol and [^{14}C]-squalene accumulation. Representative phosphorimages are shown.

(A) CHO-7 cells were treated and labeled with [^{14}C]-acetate in medium A with the following test agents for 4 hr: squalene synthase inhibitor (SSi, 150 μM), SM inhibitor (SMi, 10 μM), LDL (50 μg/ml), cholesterol complexed with methyl-β-cyclodextrin (Chol/CD, 20 μg cholesterol/ml), or 25-hydroxycholesterol (25HC, 1 μg/ml). [^{14}C]-Squalene accumulation was expressed relative to the maximal condition (Chol/CD), which was set to 1 (n = 5, +SEM).

(B) After 16 hr of growth in either LPDS (medium A) or NCS (medium C) without statin pretreatment, CHO-7 cells were labeled with [^{14}C]-acetate, and treated for 4 hr with or without Chol/CD (20 μg/ml; top panel) or LDL (50 μg/ml; bottom panel) (each n = 2).

(C) Cells in medium E (HepG2) or medium H [BE(2)C, HEK293, and fibroblasts (Fbs)] were labeled with [^{14}C]-acetate, and treated with or without Chol/CD (20 μg/ml) for 4 hr (n = 2).

(D) Statin pretreated CHO-7 cells were treated in medium B with or without Chol/CD (20 μg/ml) as indicated and labeled with [^{14}C]-acetate in medium A during treatment 2 hr prior to harvesting. Relative accumulation was calculated so that [^{14}C]-squalene + [^{14}C]-cholesterol = 1 at each time point. Error bars (±SEM) are contained within the symbols (n = 6).

(E) CHO-7 cells were treated as in (D) without radiolabeling and mRNA levels for hamster SM and HMGR determined by quantitative real-time PCR (n = 3, each performed in triplicate, ± SEM).

See also Figure S1.

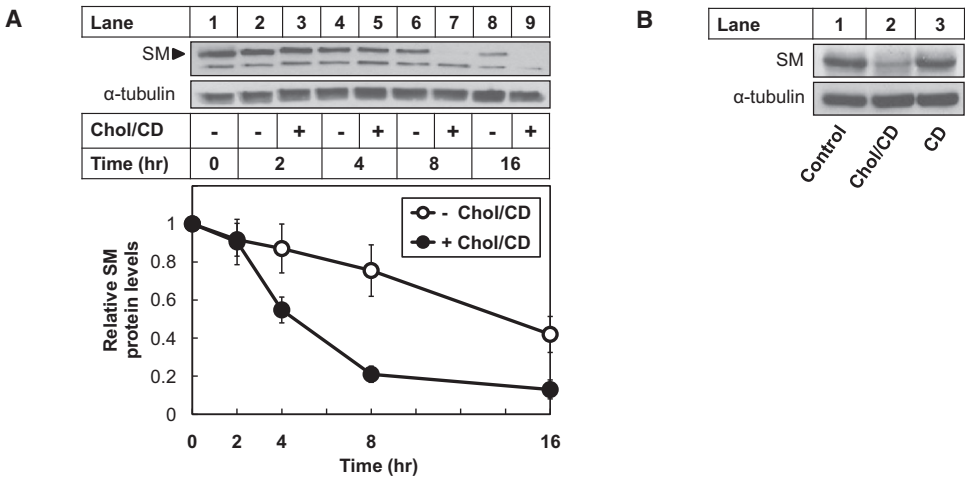

Figure 3. Cholesterol Treatment Reduces SM Protein Levels Posttranslationally in SRD-1 Cells

SRD-1 cells were statin pretreated overnight and treated as indicated in medium A containing cycloheximide (10 μg/ml) and Chol/CD (20 μg/ml) (A) or additionally with methyl-β-cyclodextrin (CD) (B) for 8 hr. Cell lysates were assayed for SM by immunoblotting (n = 3, ± SEM for A). A second band (~50 kDa) sometimes evident in the immunoblots of the endogenous protein, likely reflects partial degradation (Sakakibara et al., 1995), but not an intermediate in sterol regulated degradation, since it is unaffected by cholesterol treatment. See also Figure S2.

has been observed for HMGR (Song and DeBose-Boyd, 2004). However, the steroid-ring oxysterols 7α-hydroxycholesterol (7αHC), 7β-hydroxcholesterol (7βHC), 7-ketocholesterol (7KC), and synthetic 19-hydroxycholesterol (19HC) induced degradation (Figure 4F, lanes 2–5). Significantly, the likely cellular concentration of these oxysterols would be dramatically supraphysiological and the most potent oxysterol tested, 19HC, is not found in nature (Brown and Jessup, 1999; Brown et al., 1997). For the pathway sterols, the major methyl-sterol intermediates lanosterol and 24,25-dihydrolanosterol (24,25DHL)—the latter of which also accelerates degradation of HMGR (Lange et al., 2008; Song et al., 2005)—had no effect on SM (Figure 4G, lanes 7 and 8). 7-Dehydrocholesterol (7DHC) and lathosterol with double bonds on the steroid ring also did not reduce SM protein levels (lanes 5 and 6), whereas desmosterol which differs only by a double bond on the side chain was as effective as cholesterol (lane 4 versus lane 3). Thus, due to its much greater relative abundance compared to 7-oxygenated sterols (Brown and Jessup, 1999) or desmosterol (Yang et al., 2006), cholesterol itself appears to be the primary signal that mediates accelerated turnover of SM. The inverse curvilinear relationship between cholesterol and SM protein levels suggests the presence of a threshold required to trigger rapid degradation, approximately 15–20 μg total cholesterol/mg total protein in CHO-7 cells (Figure 4H). This threshold is close to the basal cholesterol value of ~15 μg/mg protein observed in full serum without statin pretreatment (Figure S3A), consistent with a physiological feedback role for SM degradation in control of cholesterol synthesis.

Cholesterol-Dependent Degradation of SM Is Proteasomal

Since SM is associated with the endoplasmic reticulum (ER), and the fate of many ER-bound proteins is destruction by the proteasome (Hampton, 2002), it is likely that the cholesterol-dependent degradation of SM is proteasomal. In support of this, a range of proteasomal inhibitors (ALLN, MG132, and lactacystin) preserved endogenous SM protein levels (Figure S4A). On the contrary, a lysosomal inhibitor had no effect (Figure S4B). Over a period of 8 hr, cholesterol-mediated degradation of the enzyme could be prevented with the proteasomal inhibitor MG132 (Figure 5A). As observed with endogenous hamster SM, the cholesterol-dependent reduction in ectopic human enzyme was rescued by the addition of MG132 (Figure 5B, lane 2 versus lane 4). Alternatively, glycine-alanine repeats (GAr) from Epstein-Barr virus nuclear antigen-1 were added to the ends of the human protein to provide resistance to proteasomal degradation (Sharipo et al., 1998). A single 30 amino acid repeat at the C terminus slightly increased protein levels (Figure 5C, lane 3 versus lane 1), whereas repeats on both the N and C termini blunted cholesterol-dependent degradation (lanes 5 and 6). Furthermore, in coexpression experiments with HA-tagged ubiquitin, human SM was polyubiquitinated in the presence of MG132, which was greater in the presence of cholesterol (Figure 5D, lane 4 versus lane 3). Thus, SM is degraded by the ubiquitin-proteasome system.

Importantly, in SRD-1 cells, proteasomal inhibition dramatically reduced the accumulation of squalene after 4 hr of cholesterol treatment and increased cholesterol synthesis from acetate (Figure 5E, lane 4 versus lane 3). The same effect was also observed using radiolabeled mevalonate in both SRD-1 and CHO-7 cells (Figures 5G and 5F, respectively), thus bypassing HMGR. This is consistent with the cholesterol-dependent proteasomal degradation of SM having functional consequences, by contributing to the squalene accumulation observed.

Insig and Scap Are Not Required for the Cholesterol-Dependent Degradation of SM

Sterol-dependent degradation of HMGR requires its sterol-sensing domain, which binds to the Insig retention protein, which in turn brings a ubiquitin ligase into contact with HMGR (DeBose-Boyd, 2008). To determine whether Insig is required

for degradation of SM, we observed lipid synthesis and SM turnover in SRD-15 cells. These mutant CHO cells are deficient in Insig, with no functional Insig-1 isoform, and an extremely low level of Insig-2 (Lee et al., 2005). When SRD-15 cells were treated with cholesterol, squalene still accumulated (Figure 6A) and protein degradation was still observed for both endogenous SM (Figure 6B, lane 2) and ectopic human SM (Figure 6C, left panel, lane 4). Cholesterol-dependent degradation of SM also occurred in SRD-13A cells (Rawson et al., 1999), mutant CHO cells which lack the cholesterol-sensing protein Scap and consequently do not have a functional SREBP pathway (Figure 6C, right panel, lane 2). Thus, Insig and Scap are not required for degradation of SM. Furthermore, if additional regulatory machinery is necessary, then the genes are unlikely to be strict SREBP-2 targets.

Cholesterol-Dependent Proteasomal Degradation of SM Requires Its N-Terminal Domain

The N terminus of SM, encoded by the first exon, is partially conserved in vertebrates but lacking in lower organisms (Figure 7A and Figure S5A). In addition, a recombinant truncated rat enzyme missing the first 99 residues retains full activity (Sakakibara et al., 1995). This led us to suspect that the vertebrate N-terminal region is a structurally and functionally distinct domain that may play a role in posttranscriptional regulation. We constructed a corresponding human version that is missing the N-terminal region [$\Delta(W_2\text{-}K_{100})$; Figure 7B], and examined its response to cholesterol treatment (Figure 7C). After cell fractionation, the truncated enzyme remains associated with the membrane fraction (Figure S5B, lane 5), consistent with wild-type localization. However, unlike full-length SM (WT, Figure 7C, lane 2 versus lane 1), turnover of this deletion construct was unaffected by cholesterol (lane 5 versus lane 4), and levels were further increased by addition of MG132 (lane 6 versus lane 4).

We then determined whether this lack of cholesterol-regulation of the deletion construct has functional consequences by acutely labeling transfected cells with [^{14}C]-acetate. Importantly, we observed that MOS, the product of SM, accumulates preferentially in cholesterol-treated cells transfected with the N-terminal deletion construct compared to full-length SM (Figure 7D, lane 4 versus lane 2). Accordingly, densitometric analysis showed that the squalene precursor to MOS product ratio was 30%–40% lower in the cholesterol-treated cells transfected with the truncated construct, in keeping with the failure of cholesterol to accelerate degradation of this variant.

We next prepared a complementary construct of the first 100 amino acids of epitope-tagged human SM, but it failed to express (data not shown). This may be due to the extremely hydrophobic character of this region, previously proposed to contain transmembrane domains (Ono, 2002; Sakakibara et al., 1995). However, protease protection experiments conducted in our laboratory suggested that it does not contain membrane spanning α helices. For example, an N-terminal Myc or internal FLAG epitope tag within this sequence were degraded when protease-impermeable membrane vesicles were treated with trypsin (data not shown).

To assist folding or solubilization and enable expression, we fused the first 100 amino acids (N100) to green fluorescent protein (N100-GFP) or glutathione *S*-transferase (N100-GST) under the control of the TK promoter (Figure 7B). Despite the apparent absence of membrane spanning α helices, the chimeric fusion protein was still membrane associated (Figure S5B, right panel, lane 2). Importantly, turnover of both heterologous fusion constructs was robustly regulated by cholesterol (Figure 7E, lane 4 versus lane 3; Figure S5E, lane 2 versus lane 1), whereas expression of either GFP or GST alone was unaffected by cholesterol treatment (data not shown). When the full-length protein and truncated chimera were co-transfected, cholesterol-dependent turnover of each was also unaffected (Figure 7E, lane 6 versus lane 5). This was surprising in light of the marked blunting of regulation seen for the CMV system earlier, because expression of the TK-driven truncated fusion protein (N100-GFP) was much higher than the full-length non-fusion protein (data not shown).

A pulse-chase approach, which permits the study of protein degradation without the use of cycloheximide, confirmed that Chol/CD treatment accelerates degradation of the N100-GST (Figure 7F) and suggests a comparable half-life ($\sim$3 hr) to that seen in the cycloheximide-containing studies on full-length endogenous SM ($\sim$4 hr in Figures 3A and 5A). Without added cholesterol, the N100-GST appeared remarkably stable over the 8 hr. Cholesterol began to degrade this truncated version of SM by 2 hr (Figure 7F), in line with the timing observed for squalene accumulation (Figures 1D and 2B). This pulse-chase approach was not possible for endogenous SM due to lack of an appropriate antibody for immunoprecipitation.

Coexpression of a chain-terminating K48R ubiquitin mutant through fusion to N100-GFP blunted cholesterol-dependent degradation and increased SM protein levels compared to wild-type ubiquitin (Figure S5F), again implicating the ubiquitin-proteasome system. Moreover, GST pull-down of the N100-GST chimera coexpressed with HA-tagged ubiquitin revealed clear cholesterol-dependent polyubiquitination (Figure 7G, lane 1 versus lane 2), which was observed as early as one hour after cholesterol treatment (Figure S5G).

Together, these data suggest that the N-terminal region forms a regulatory domain, which is necessary and sufficient for post-translational regulation of SM by the proteasome, and which in turn may help to regulate flux through the cholesterol biosynthetic pathway.

DISCUSSION

Cholesterol synthesis is controlled at multiple levels, including transcriptionally by the SREBPs (Goldstein et al., 2006), and posttranscriptionally, notably at HMGR (DeBose-Boyd, 2008). Here, we present evidence that cholesterol can stimulate with considerable specificity the proteasomal degradation of SM, a neglected enzyme beyond HMGR. Consistent with this, cholesterol treatment caused the nontoxic isoprenoid squalene to accumulate in a variety of cell lines (Figure 1), preceding transcriptional downregulation of SM. Indeed, cholesterol-dependent squalene accumulation was also observed in mutant cells lacking transcriptional regulation by SREBP-2 (Figure 2). At the posttranslational level, this was accompanied by a reduction in endogenous SM protein levels (Figure 3). In an example of end-product inhibition, turnover was accelerated by cholesterol itself, rather than methylated sterols or side-chain oxysterols (Figure 4). Cholesterol-dependent degradation of SM also

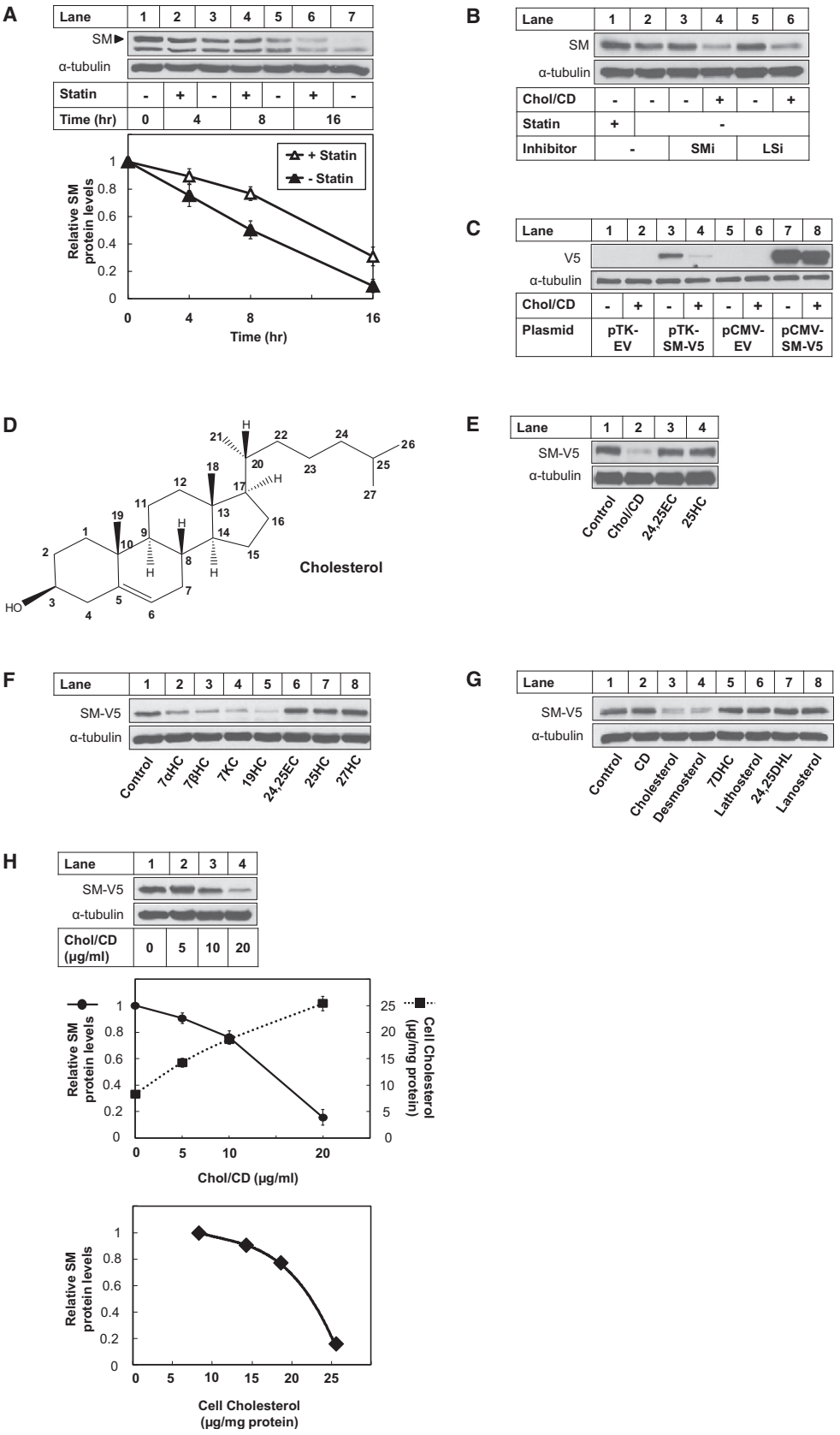
A
Lane 1 2 3 4 5 6 7
SM
α-tubulin
Statin - + - + - + -
Time (hr) 0 4 8 16
+ Statin
- Statin
Relative SM protein levels
Time (hr)
B
Lane 1 2 3 4 5 6
SM
α-tubulin
Chol/CD - - - + - +
Statin + -
Inhibitor - SMi LSi
C
Lane 1 2 3 4 5 6 7 8
V5
α-tubulin
Chol/CD - + - + - + - +
Plasmid pTK-EV pTK-SM-V5 pCMV-EV pCMV-SM-V5
D
Cholesterol
E
Lane 1 2 3 4
SM-V5
α-tubulin
Control
Chol/CD
24,25EC
25HC
F
Lane 1 2 3 4 5 6 7 8
SM-V5
α-tubulin
Control
7αHC
7βHC
7KC
19HC
24,25EC
25HC
27HC
G
Lane 1 2 3 4 5 6 7 8
SM-V5
α-tubulin
Control
CD
Cholesterol
Desmosterol
7DHC
Lathosterol
24,25DHL
Lanosterol
H
Lane 1 2 3 4
SM-V5
α-tubulin
Chol/CD (μg/ml) 0 5 10 20
Relative SM protein levels
Cell Cholesterol (μg/mg protein)
Chol/CD (μg/ml)
Relative SM protein levels
Cell Cholesterol (μg/mg protein)

required the ubiquitin-proteasome system: protein levels were rescued through proteasomal inhibition with MG132, and polyubiquitination increased on cholesterol treatment (Figure 5). This mechanism did not require Insig or Scap (Figure 6) but was mediated by the N-terminal region of human SM, which also conferred sterol-regulated turnover on heterologous fusion proteins (Figure 7). Importantly, MG132 reversed the accumulation of squalene, suggesting that accelerated proteasomal degradation of SM may help to acutely control flux through the cholesterol biosynthetic pathway.

Clearly, while this mechanism may be a second example of regulated degradation for the control of cholesterol synthesis, it is distinct from the well-characterized ER-associated degradation of HMGR: SM lacks the five transmembrane sterol-sensing domain and its degradation is not mediated by Insig, 24,25-dihydrolanosterol, or side-chain oxysterols such as 27HC. Indeed, the sterol specificity of SM degradation is also strikingly different for that previously shown to inhibit SREBP processing, and/or bind to Scap or Insig (summarized in Figure S3B).

What might be the evolutionary advantage of having an additional posttranslational control point for regulating cholesterol synthesis beyond HMGR? Transcriptional downregulation of the SREBP pathway is relatively slow, with mRNA levels of target genes only appreciably decreasing hours after treatment (Figure 1E), potentially leaving active enzyme with a relatively long half-life. More rapid shutdown of cholesterol synthesis requires posttranscriptional control, such as the well-documented proteasome-mediated degradation of HMGR (DeBose-Boyd, 2008). However, HMGR activity can vary widely (DeBose-Boyd, 2008), such that sterol synthesis could be difficult to dampen in a timely manner. Moreover, some HMGR activity is needed for isoprenoid production (Brown and Goldstein, 1980). In contrast, SM appears to have much lower activity than HMGR (Hidaka et al., 1990) and is committed to sterol production, making it suitable for rapid modulation of the cholesterol biosynthetic pathway independently from isoprenoid synthesis. We propose a model whereby the mevalonate pathway is controlled rapidly and segmentally at HMGR and SM (Figure 7H). One situation in which this could be useful would be to respond to a sudden influx of exogenous cholesterol while the demand for isoprenoids such as farnesol or geranylgeraniol remains high. This argument is consistent with the observation that the physiologically relevant cholesterol molecule itself appears to be the major signal for SM degradation (Figure 4).

To begin delineating the mechanism of accelerated degradation of SM, we hypothesized that the N terminus was involved, based on its lack of requirement for catalytic activity (Sakakibara et al., 1995) and on its evolutionary conservation (Figure 7A). This region is particularly well-conserved between birds and mammals, suggesting that this mechanism may have evolved to assist cholesterol regulation in higher animals. Indeed, we showed that the first 100 amino acids (comprising 17% of the protein) was sufficient to mediate cholesterol-regulated turnover of GST or GFP (Figure 7), when GFP alone for example is otherwise remarkably stable (Corish and Tyler-Smith, 1999). Although the membrane topology of SM is currently unknown, our preliminary investigations have determined that the hydrophobic N-terminal domain is sufficient but not necessary for membrane association (Figure S5B). This region contains the short sequences "YFY" and "LGIA" in close proximity, near-identical to motifs found in transmembrane helices of the sterol-sensing domain of HMGR and Scap, shown to be functionally important for Insig binding (Sever et al., 2003; Yabe et al., 2002; Yang et al., 2002). The YIYF peptide has also been suggested to recruit cholesterol on the basis of phase transition experiments (Epand, 2006). However, mutation of the tyrosines to serine or the leucine to alanine did not abolish regulation, although they appeared to destabilize the protein (Figure S5C, lanes 3 and 4 of each panel). It is not known whether regulated degradation requires direct binding of cholesterol to the N terminus. Mutation of a single tyrosine from a further motif, fulfilling the CRAC cholesterol binding consensus sequence (Epand, 2006), also had no effect on regulation (Figure S5C, left panel, lanes 5 and 6). Furthermore, it is not known whether regulated degradation requires a conformational change mediated by altered membrane structure or requires a second sensing protein. The blunted regulation seen for the CMV-driven expression vector (Figure 4C and data not shown) hints at the presence of additional regulatory proteins. By contrast, competition for a limiting factor(s) did not appear to occur when we cotransfected full-length SM and the massively overexpressed N100-GFP fusion protein (Figure 7E). Thus, this question remains an area of uncertainty.

Our preliminary experiments using protease protection are consistent with the N-terminal domain being accessible to the cytoplasmic ubiquitin-proteasome system. However, our numerous attempts at identifying an ubiquitination site for SM using site-directed mutagenesis have been unsuccessful to date. This involved mutating groups of lysines to arginine, including selected conserved residues (Figure S5D), or all from

Figure 4. Degradation of SM Is Accelerated by Cholesterol Rather Than Side-Chain Oxysterols

(A and B) SRD-1 cells were statin pretreated overnight and treated as indicated in medium A containing cycloheximide (10 μg/ml) and either statin (compactin, 5 μM, thus identical to medium B), SM inhibitor (SMi, 10 μM), lanosterol synthase inhibitor (LSi, 10 μM), and/or Chol/CD (20 μg/ml). Cell lysates were assayed for SM by immunoblotting (n = 4, ± SEM for A).

(D) Cholesterol structure with carbons numbered.

(C and E–H) CHO-7 cells were transfected with 1 μg empty vector (EV), plasmid encoding human SM constructs as indicated (C) or pTK-SM-V5 (E–H). After overnight statin pretreatment, CHO-7 cells were treated for 8 hr in medium B containing cycloheximide (10 μg/ml) with or without the following: Chol/CD (20 μg/ml or as indicated), 24(*S*),25-epoxycholesterol (24,25EC, 1 μg/ml), or 25-hydroxycholesterol (25HC, 1 μg/ml) (C, E, and H) or an equivalent concentration of CD alone or CD complexed with the sterols (20 μg/ml) 7α-hydroxycholesterol (7αHC), 7β-hydroxycholesterol (7βHC), 7-ketocholesterol (7KC), 19-hydroxycholesterol (19HC), 24,25EC, 25HC, 27-hydroxycholesterol (27HC), cholesterol, desmosterol, 7-dehydrocholesterol (7DHC), lathosterol, 24,25-dihydrolanosterol (24,25DHL), or lanosterol (F and G). SM-V5 protein was analyzed by immunoblotting (each n = 4).

(H) CHO-7 cells were transfected and treated as above, except with varying concentrations of Chol/CD (0–20 μg/ml) for 8 hr (n = 8). Total cellular cholesterol levels were measured in parallel experiments (n = 3). The error bars (±SEM) presented are sometimes contained within the symbols.

See also Figure S3.

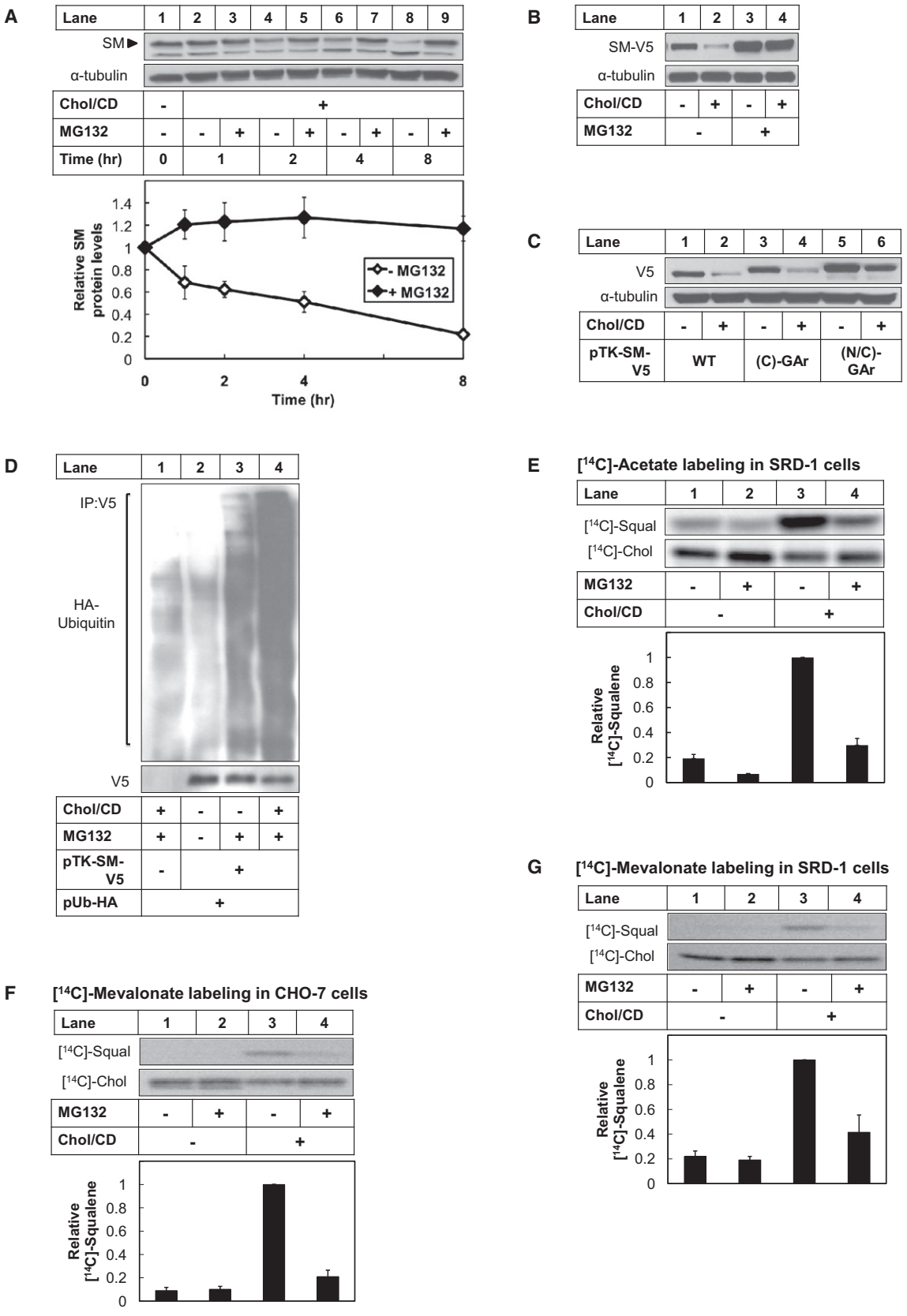
A
Lane 1 2 3 4 5 6 7 8 9
SM
α-tubulin
Chol/CD - +
MG132 - - + - + - + - +
Time (hr) 0 1 2 4 8
Relative SM protein levels
1.4 1.2 1 0.8 0.6 0.4 0.2 0
- MG132
+ MG132
0 2 4 8
Time (hr)
B
Lane 1 2 3 4
SM-V5
α-tubulin
Chol/CD - + - +
MG132 - +
C
Lane 1 2 3 4 5 6
V5
α-tubulin
Chol/CD - + - + - +
pTK-SM-V5 WT (C)-GAr (N/C)-GAr
D
Lane 1 2 3 4
IP:V5
HA-Ubiquitin
V5
Chol/CD + - - +
MG132 + - + +
pTK-SM-V5 - +
pUb-HA +
E
[14C]-Acetate labeling in SRD-1 cells
Lane 1 2 3 4
[14C]-Squal
[14C]-Chol
MG132 - + - +
Chol/CD - +
Relative [14C]-Squalene
1 0.8 0.6 0.4 0.2 0
F
[14C]-Mevalonate labeling in CHO-7 cells
Lane 1 2 3 4
[14C]-Squal
[14C]-Chol
MG132 - + - +
Chol/CD - +
Relative [14C]-Squalene
1 0.8 0.6 0.4 0.2 0
G
[14C]-Mevalonate labeling in SRD-1 cells
Lane 1 2 3 4
[14C]-Squal
[14C]-Chol
MG132 - + - +
Chol/CD - +
Relative [14C]-Squalene
1 0.8 0.6 0.4 0.2 0

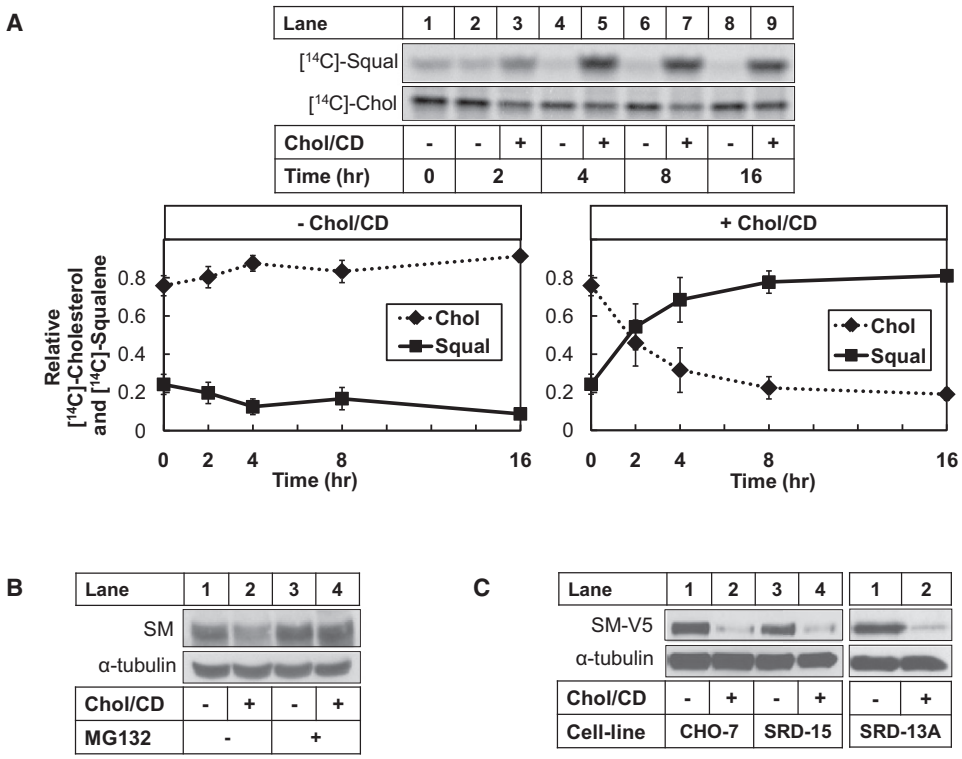

Figure 6. Insig and Scap Are Not Required for Accelerated Degradation of SM

(A) SRD-15 cells, deficient in Insig, were treated as in Figure 1D (n = 5, ± SEM).

(B) SRD-15 cells were treated as in Figure 5A. Cell lysates were assayed for SM by immunoblotting (n = 4).

(C) SRD-13A cells are deficient in Scap. The indicated cell lines were transfected with 1 μg of pTK-SM-V5, statin pretreated overnight, and treated in medium B containing cycloheximide (10 μg/ml) with or without Chol/CD (20 μg/ml) for 8 hr. SM-V5 protein was analyzed by immunoblotting (each n = 2).

the first 100 amino acids of the full-length protein (data not shown) and heterologous fusions (Figure S5E), which all retained cholesterol-regulated turnover. These data suggest that a specific regulated ubiquitination site may be unnecessary and/or that ubiquitination may occur on the N-terminal amino group.

Our studies suggest that accelerated SM degradation in response to cholesterol has functional consequences, by contributing to flux control through the cholesterol synthesis pathway. This is based on proteasomal inhibition reversing sterol-dependent accumulation of squalene, even when employing radiolabeled mevalonate (to bypass HMGR). Moreover, cholesterol fails to accelerate degradation of the SM construct lacking the N-terminal domain, with a concomitant greater flux through SM (as indicated by increased formation of the product MOS). While generally comparable, the time course of squalene accumulation did not exactly mirror falling SM protein levels (cf. Figures 2B and 3A). However, it is noteworthy that in experiments without cycloheximide, cholesterol-mediated effects on the N-terminal domain were observed earlier (at 1 hr, with ubiquitination [Figure S5G], and at 2 hr, with a pulse-chase approach [Figure 7F]). This more rapid timing is compatible with that observed for squalene accumulation (obtained without cycloheximide). It is possible that cycloheximide may alter the kinetics of SM degradation, as has been noted previously for HMGR (Chun et al., 1990). Nevertheless, there is a chance that other posttranscriptional mechanisms may be involved in the control of mammalian SM activity, which remain to be revealed.

Figure 5. Regulated Turnover of SM Is Mediated by the Ubiquitin-Proteasome System

(A) SRD-1 cells were statin pretreated overnight and treated in medium B containing cycloheximide (10 μg/ml), Chol/CD (20 μg/ml), and MG132 (10 μM), as indicated. Cell lysates were assayed for SM by immunoblotting (n = 3, ± SEM).

(B and C) CHO-7 cells were transfected with 1 μg of plasmid as indicated, statin pretreated and treated as in (A) for 8 hr (n = 4 each). The SM constructs in (C) contain glycine-alanine repeats at the C and/or N termini of wild-type (WT) SM-V5 as indicated. Cell lysates were assayed for SM-V5 by immunoblotting (n = 2).

(D) CHO-7 cells (in 6 cm dishes) were transfected with 1.5 μg of pTK-SM-V5 and 0.5 μg of pMT123 (pUb-HA, HA-tagged ubiquitin), statin pretreated, treated in medium B with or without Chol/CD (20 μg/ml) and MG132 (10 μM) as indicated. The SM-V5 was immunoprecipitated from cell lysates. Immunoprecipitated pellets were assayed for SM-V5 or HA-ubiquitin by immunoblotting (n = 2).

(E–G) Statin pretreated SRD-1 (E and G) or CHO-7 (F) cells were treated in medium A with or without Chol/CD (20 μg/ml) and/or MG132 (10 μM), and labeled with [14C]-acetate (E) or [14C]-mevalonate (F and G) for 4 hr. [14C]-Squalene accumulation was expressed relative to the maximal condition (Chol/CD), which was set to 1 (n = 4 in E, 5 in F, and 3 in G, +SEM).

See also Figure S4.

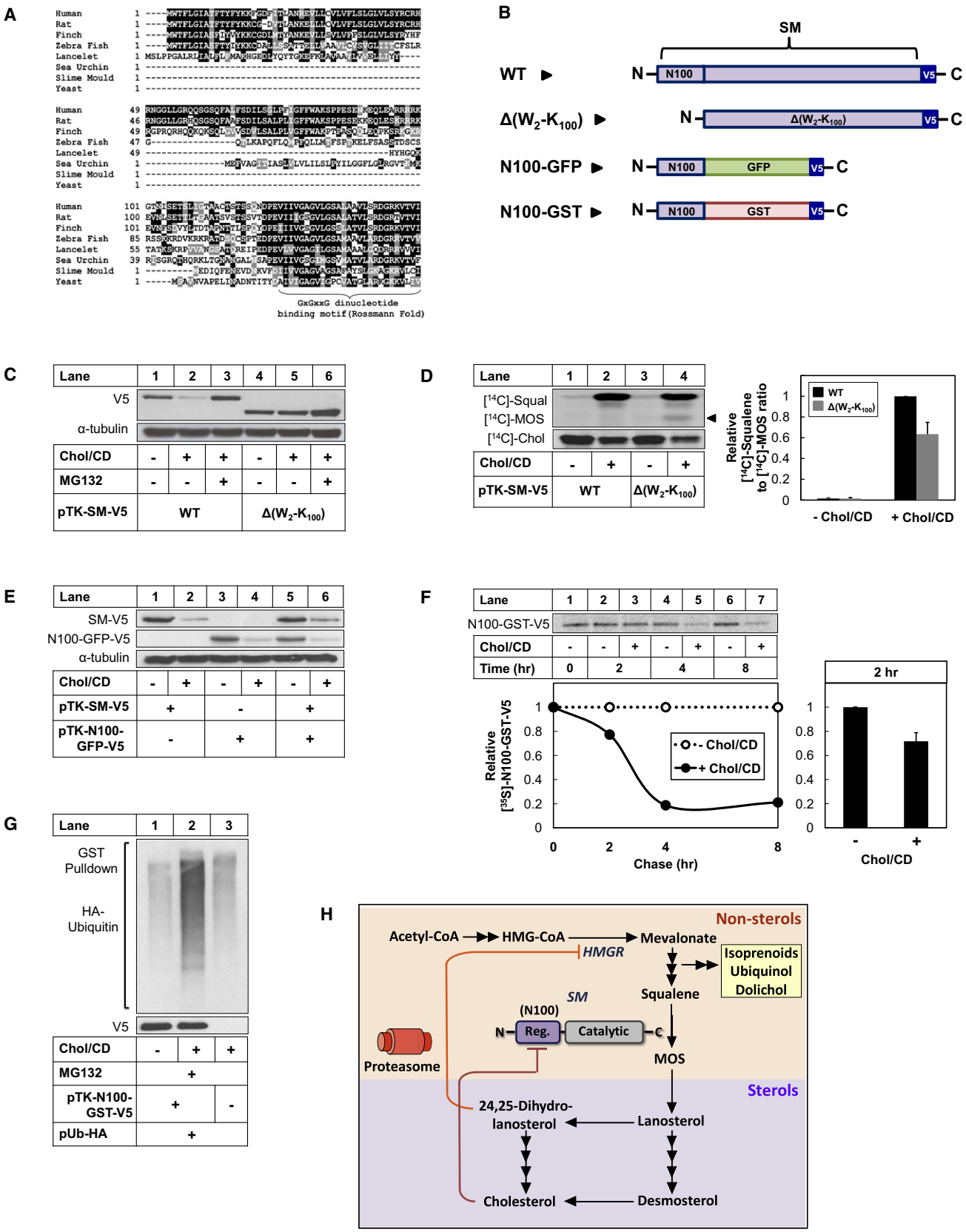
A
Human
Rat
Finch
Zebra Fish
Lancelet
Sea Urchin
Slime Mould
Yeast
GxGxxG dinucleotide binding motif (Rossmann Fold)
B
SM
WT
Δ(W2-K100)
N100-GFP
N100-GST
N100
GFP
GST
V5
C
Lane
V5
α-tubulin
Chol/CD
MG132
pTK-SM-V5
WT
Δ(W2-K100)
D
[14C]-Squal
[14C]-MOS
[14C]-Chol
Relative [14C]-Squalene to [14C]-MOS ratio
- Chol/CD
+ Chol/CD
E
SM-V5
N100-GFP-V5
pTK-N100-GFP-V5
F
N100-GST-V5
Time (hr)
Relative [35S]-N100-GST-V5
Chase (hr)
2 hr
G
GST Pulldown
HA-Ubiquitin
pTK-N100-GST-V5
pUb-HA
H
Non-sterols
Acetyl-CoA
HMG-CoA
Mevalonate
HMGR
Isoprenoids
Ubiquinol
Dolichol
Squalene
SM
(N100)
Reg.
Catalytic
Proteasome
MOS
Sterols
24,25-Dihydro-lanosterol
Lanosterol
Cholesterol
Desmosterol

Although Chol/CD may be considered a nonphysiological mode of cholesterol delivery, it was employed for most experiments in this paper as it produced a more robust squalene accumulation than LDL (illustrated in Figures 1A and 1B and Figure S1B). Furthermore, Chol/CD also offers advantages in that is a far "cleaner" source of cholesterol than LDL (i.e., devoid of other lipids) and delivers cholesterol directly, hence avoiding the complications of having first to pass through the endosomal/lysosomal system. However, it should be noted that increased SM degradation was observed in full serum compared with cholesterol-depleted serum (Figure S2), consistent with the physiological relevance of this mechanism.

In conclusion, our results suggest yet another layer of complexity in the control of cholesterol synthesis. In an example of end-product inhibition, cholesterol feeds back to stimulate the proteasomal degradation of SM in a mechanism that is distinct from that previously established for HMGR. This raises the possibility that SM may constitute a second important control point in cholesterol synthesis, serving as a reminder that flux control of metabolic pathways tends to be shared by multiple enzymes (Thomas and Fell, 1998), which could facilitate flexible control of different intermediates. However, to what extent degradation of SM normally regulates cholesterol synthesis in vivo remains to be determined. Our findings may explain the often observed positive association between serum levels of squalene and cholesterol in humans, under a variety of pathophysiological and pharmacological conditions (e.g., Rajaratnam et al., 1999). Furthermore, our work may have important implications for human health and disease, notably in relation to cardiovascular disease, but also other conditions (e.g., neurodegenerative diseases and certain cancers) in which cholesterol has also been implicated. Moreover, this work may stimulate interest in SM as a potential therapeutic target for cholesterol-related diseases (Chugh et al., 2003).

EXPERIMENTAL PROCEDURES

A complete description of materials, cell culture procedures and media (A–I), primers, and other methods is available in the Supplemental Experimental Procedures.

Cell Culture

In general, various CHO cell lines were employed (kind gifts of Goldstein, Brown, and DeBose-Boyd, University of Texas Southwestern, Dallas). Unless otherwise stated, cells were statin pretreated overnight (16 hr) to deplete sterols through incubation in medium containing LPDS, the HMGR inhibitor compactin (5 μm), and a low level of mevalonate (50 μm) that allows synthesis of essential non-sterol isoprenoids but not of cholesterol (Hartman et al., 2010). After statin pretreatment, cells were washed once with PBS, which was sufficient to remove any residual compactin. For treatment, the media was refreshed to include test agents as described in the figure legends for the times indicated, followed by cell harvesting for the assays described below.

Metabolic Labeling of Squalene and Cholesterol

Accumulation of [^{14}C]-squalene and [^{14}C]-cholesterol were determined by radio-TLC (thin-layer chromatography) as described (Wong et al., 2008) with minor modifications (see the Supplemental Experimental Procedures for details). After statin pretreatment, cells were metabolically labeled with 1 μCi/well [^{14}C]-acetate or [^{14}C]-mevalonate added to the existing media for the last 2 or 4 hr of treatment, as indicated. Cell lysates were subjected to alkaline saponification followed by neutral lipid extraction. Bands corresponding to authentic standards were visualized with a FLA-5100 phosphorimager (Fujifilm), and their relative intensities were quantified with Sciencelab ImageGauge 4.0 Software (Fujifilm).

Quantitative Real-Time PCR

As previously described (Wong et al., 2008), RNA was harvested in triplicate with TRIzol reagent and reverse transcribed to yield complementary DNA (cDNA) with the SuperScript III First Strand cDNA Synthesis kit (Invitrogen), and mRNA levels determined relative to the housekeeping gene by quantitative real-time PCR using SYBR Green and a Corbett Rotorgene 3000. Primers were directed against SM (*SQLE*) and HMGR (*HMGCR*), with porphobilinogen deaminase (*Pbgd*) as the housekeeping gene.

Figure 7. The N-Terminal Domain of Human SM Is Necessary and Sufficient for Cholesterol-Dependent Proteasomal Degradation

(A) Multiple sequence alignment of the first ~150 amino acids of SM for selected species.

(B) Schematic of SM deletion and fusion constructs.

(C, D, and E) CHO-7 cells were transfected as indicated. After statin pretreatment, cells were treated in medium B containing cycloheximide (10 μg/ml), with or without Chol/CD (20 μg/ml), and/or MG132 (10 μM) for 8 hr. V5-tagged SM constructs were analyzed by immunoblotting.

(C) One microgram pTK-SM-V5 (WT) or pTK-SM-Δ(W_2-K_{100})-V5 [Δ(W_2-K_{100})] (n = 2).

(D) Statin-pretreated CHO-7 cells transfected the previous day with 1 μg DNA as in (C) were labeled with [^{14}C]-acetate in medium A and treated with or without Chol/CD (20 μg/ml) for 4 hr. Cells were assayed for accumulation of [^{14}C]-cholesterol, [^{14}C]-squalene, and [^{14}C]-2,3-monooxidosqualene (MOS). The [^{14}C]-MOS band is indicated with an arrow. The [^{14}C]-squalene to [^{14}C]-MOS ratio was expressed relative to the maximal condition (cells transfected with pTK-SM-V5 and treated with Chol/CD), which was set to 1. For the Chol/CD conditions, the Δ(W_2-K_{100}) construct produced a lower [^{14}C]-squalene to [^{14}C]-MOS ratio than the wild-type (WT) construct ($p < 0.05$ by t test; n = 5, +SEM).

(E) 0.5 μg pTK-SM-V5 (WT) and/or 0.5 μg pTK-SM-N100-GFP-V5 (N100-GFP) (n = 3).

(F) CHO-7 cells were transfected with 0.25 μg of pTK-SM-N100-GST-V5 (N100-GST). After statin pretreatment, cells were pulsed for 3 hr with [^{35}S]-methionine/cysteine and then chased in medium B with or without Chol/CD (20 μg/ml) for 0–8 hr. [^{35}S]-N100-GST protein was pulled down with glutathionine sepharose, analyzed by SDS-PAGE, and the band visualized by phosphorimaging. For the image shown, densitometric values were plotted for the +Chol/CD conditions. The –Chol/CD values, which did not change over the 8 hr, were each set to 1. Right-hand panel: Cholesterol significantly degraded N100-GST at 2 hr ($p < 0.05$ by t test; n = 4, +SEM).

(G) CHO-7 cells (in 10 cm dishes) were transfected with 1.5 μg pTK-SM-N100-GST-V5 (N100-GST) and 0.5 μg pMT123 (pUb-HA, HA-tagged ubiquitin). After statin pretreatment, cells were treated in medium B with or without Chol/CD (20 μg/ml) and MG132 (10 μM) for 4 hr. N100-GST protein was pulled down with glutathionine sepharose and immunoblotted for V5 (N100-GST) and HA-ubiquitin (n = 2).

(H) Segmental control of the mevalonate pathway. Sterol-dependent, posttranslational control of the mevalonate pathway is mediated in large part by the ubiquitin-proteasome system. 3-Hydroxy-3-methylglutaryl-coenzyme A reductase (HMGR) is degraded in response to 24,25-dihydrolanosterol and side-chain oxysterols (not shown), which will consequently also reduce flux into the nonsterol branch of the pathway. In contrast, turnover of squalene monooxygenase (SM) is accelerated by the end product, cholesterol itself, specifically inhibiting sterol production. This cholesterol-dependent degradation of SM requires its N-terminal 100 amino acids, here designated as the regulatory domain (Reg.), which is separate from the catalytic portion of the enzyme.

See also Figure S5.

Immunoblot Analysis

Immunoblot analysis was performed as described (Kristiana et al., 2010) with minor modifications. Cells were lyzed in 100 μl 10% (w/v) SDS with 5 μl protease inhibitor cocktail. Samples (usually 40 μg of protein) were analyzed by 10% SDS-PAGE and immunoblotted with the following antibodies: anti-V5 (1:10000), anti-SM (1:5000), anti-HA (1:10000), and anti-α-tubulin (1:200000). The observed endogenous protein bands migrated according to their calculated molecular weight: 64 kDa for SM and 50 kDa for α-tubulin. The relative intensities of bands were quantified by densitometry with ImageJ Software (1.36b).

Transfection

CHO cells in 6-well plates (unless otherwise stated) were grown in medium A (but without antibiotics) and transfected the following day with Lipofectamine LTX reagent (Invitrogen) according to the manufacturer's instructions, with a ratio of 1 μg of DNA:4 μl of transfection reagent. DNA was equalized with empty vector between different conditions. After 24 hr transfection, cells were statin pretreated overnight and then treated as indicated.

Cholesterol Mass Determination

Cells were washed, harvested in modified RIPA buffer (1.0% IGEPAL CA-630, 0.1% SDS, 0.5% sodium deoxycholate, 1 mM sodium orthovanadate, 150 mM NaCl, 1 mM Na EDTA, 20 mM Tris-HCl [pH 7.4]) and passed through an 18G needle 20 times. Total cellular cholesterol content was determined using the Amplex Red Cholesterol assay kit (Invitrogen), according to the manufacturer's instructions (with an Fmax microplate spectrofluorometer [Molecular Devices, CA], excitation $\lambda = 544$ nm, emission $\lambda = 590$ nm), and expressed relative to protein (measured by the Bicinchoninic Acid assay, Pierce).

Ubiquitination of Human SM

After transfection and treatment (as indicated in the figure legends), CHO-7 cells were lyzed in modified RIPA buffer (described above) supplemented with N-ethylmaleimide (10 mM), protease inhibitor cocktail, and ALLN (25 μg/ml). Lysates with equal cell protein were immunoprecipitated with monoclonal anti-V5-conjugated Dynabeads (Invitrogen), according to the manufacturer's instructions. Pull-down of the N100-GST fusion protein from lysates with equal cell protein was achieved using glutathione sepharose beads. Pellets were subjected to 7.5% SDS-PAGE, followed by immunoblot analysis with anti-V5 (for SM) and anti-HA (for ubiquitin) antibodies.

Metabolic Labeling of N100-GST with [^{35}S]-Methionine/Cysteine

CHO-7 cells were transiently transfected as indicated in the figure legend. After statin pretreatment, cells were labeled in methionine-free medium (Invitrogen) supplemented with 5 μM compactin and 50 μM mevalonate containing 250 μCi/ml [^{35}S]-Protein Labeling Mix (Perkin Elmer) for 3 hr, then washed and chased in medium B containing 2 mM methionine and cysteine with or without Chol/CD, for 0–8 hr. [^{35}S]-labeled N100-GST was pulled down from lysates with equal cell protein using glutathione sepharose beads, and pellets were subjected to 4%–20% or 10% SDS-PAGE. Bands were visualized by phosphorimaging, and their relative intensities were quantified with Sciencelab ImageGauge 4.0 Software (Fujifilm).

Data Presentation

Unless otherwise indicated, values are normalized to the vehicle-treated control condition. Quantitative data are presented as averages and all error bars represent the standard error of the mean (SEM). Other data are comprised or representative of at least n separate experiments, as noted in the figure legends.

SUPPLEMENTAL INFORMATION

Supplemental Information includes Supplemental Experimental Procedures and five figures and can be found with this article online at doi:10.1016/j.cmet.2011.01.015.

ACKNOWLEDGMENTS

We thank Jenny Wong for her preliminary work on this project and constructing the pCMV-SM-V5 plasmid, and members of the Brown Lab and Ingrid Gelissen for critically reviewing this manuscript. We thank Maaike Kockx for her valuable assistance with the [^{35}S] labeling experiments. The Brown Lab was supported by grants from the National Health and Medical Research Council (568619), the Prostate Cancer Foundation of Australia (PR36), and the University of New South Wales (UNSW Goldstar Award). J.S. is supported by an Australian Postgraduate Award.

Received: May 24, 2010
Revised: October 22, 2010
Accepted: January 20, 2011
Published: March 1, 2011

REFERENCES

Abe, I., Seki, T., Umehara, K., Miyase, T., Noguchi, H., Sakakibara, J., and Ono, T. (2000). Green tea polyphenols: novel and potent inhibitors of squalene epoxidase. Biochem. Biophys. Res. Commun. *268*, 767–771.

Adams, C.M., Reitz, J., De Brabander, J.K., Feramisco, J.D., Li, L., Brown, M.S., and Goldstein, J.L. (2004). Cholesterol and 25-hydroxycholesterol inhibit activation of SREBPs by different mechanisms, both involving SCAP and Insigs. J. Biol. Chem. *279*, 52772–52780.

Brown, M.S., and Goldstein, J.L. (1980). Multivalent feedback regulation of HMG CoA reductase, a control mechanism coordinating isoprenoid synthesis and cell growth. J. Lipid Res. *21*, 505–517.

Brown, A.J., and Jessup, W. (1999). Oxysterols and atherosclerosis. Atherosclerosis *142*, 1–28.

Brown, A.J., Leong, S.L., Dean, R.T., and Jessup, W. (1997). 7-Hydroperoxycholesterol and its products in oxidized low density lipoprotein and human atherosclerotic plaque. J. Lipid Res. *38*, 1730–1745.

Chugh, A., Ray, A., and Gupta, J.B. (2003). Squalene epoxidase as hypocholesterolemic drug target revisited. Prog. Lipid Res. *42*, 37–50.

Chun, K.T., Bar-Nun, S., and Simoni, R.D. (1990). The regulated degradation of 3-hydroxy-3-methylglutaryl-CoA reductase requires a short-lived protein and occurs in the endoplasmic reticulum. J. Biol. Chem. *265*, 22004–22010.

Corish, P., and Tyler-Smith, C. (1999). Attenuation of green fluorescent protein half-life in mammalian cells. Protein Eng. *12*, 1035–1040.

DeBose-Boyd, R.A. (2008). Feedback regulation of cholesterol synthesis: sterol-accelerated ubiquitination and degradation of HMG CoA reductase. Cell Res. *18*, 609–621.

Eilenberg, H., and Shechter, I. (1984). A possible regulatory role of squalene epoxidase in Chinese hamster ovary cells. Lipids *19*, 539–543.

Epand, R.M. (2006). Cholesterol and the interaction of proteins with membrane domains. Prog. Lipid Res. *45*, 279–294.

Goldstein, J.L., DeBose-Boyd, R.A., and Brown, M.S. (2006). Protein sensors for membrane sterols. Cell *124*, 35–46.

Gonzalez, R., Carlson, J.P., and Dempsey, M.E. (1979). Two major regulatory steps in cholesterol synthesis by human renal cancer cells. Arch. Biochem. Biophys. *196*, 574–580.

Gupta, N., and Porter, T.D. (2001). Garlic and garlic-derived compounds inhibit human squalene monooxygenase. J. Nutr. *131*, 1662–1667.

Hampton, R.Y. (2002). ER-associated degradation in protein quality control and cellular regulation. Curr. Opin. Cell Biol. *14*, 476–482.

Hartman, I.Z., Liu, P., Zehmer, J.K., Luby-Phelps, K., Jo, Y., Anderson, R.G., and DeBose-Boyd, R.A. (2010). Sterol-induced dislocation of 3-hydroxy-3-methylglutaryl coenzyme A reductase from endoplasmic reticulum membranes into the cytosol through a subcellular compartment resembling lipid droplets. J. Biol. Chem. *285*, 19288–19298.

Hidaka, Y., Satoh, T., and Kamei, T. (1990). Regulation of squalene epoxidase in HepG2 cells. J. Lipid Res. *31*, 2087–2094.

Horton, J.D., Shah, N.A., Warrington, J.A., Anderson, N.N., Park, S.W., Brown, M.S., and Goldstein, J.L. (2003). Combined analysis of oligonucleotide microarray data from transgenic and knockout mice identifies direct SREBP target genes. Proc. Natl. Acad. Sci. USA *100*, 12027–12032.

Kristiana, I., Sharpe, L.J., Catts, V.S., Lutze-Mann, L.H., and Brown, A.J. (2010). Antipsychotic drugs upregulate lipogenic gene expression by disrupting intracellular trafficking of lipoprotein-derived cholesterol. Pharmacogenomics J. *10*, 396–407.

Lange, Y., Ory, D.S., Ye, J., Lanier, M.H., Hsu, F.F., and Steck, T.L. (2008). Effectors of rapid homeostatic responses of endoplasmic reticulum cholesterol and 3-hydroxy-3-methylglutaryl-CoA reductase. J. Biol. Chem. *283*, 1445–1455.

Lee, P.C., Sever, N., and Debose-Boyd, R.A. (2005). Isolation of sterol-resistant Chinese hamster ovary cells with genetic deficiencies in both Insig-1 and Insig-2. J. Biol. Chem. *280*, 25242–25249.

Metherall, J.E., Goldstein, J.L., Luskey, K.L., and Brown, M.S. (1989). Loss of transcriptional repression of three sterol-regulated genes in mutant hamster cells. J. Biol. Chem. *264*, 15634–15641.

Nagai, M., Sakakibara, J., Nakamura, Y., Gejyo, F., and Ono, T. (2002). SREBP-2 and NF-Y are involved in the transcriptional regulation of squalene epoxidase. Biochem. Biophys. Res. Commun. *295*, 74–80.

Ono, T. (2002). The first step of oxygenation in cholesterol biosynthesis. Biochem. Biophys. Res. Commun. *292*, 1283–1288.

Rajaratnam, R.A., Gylling, H., and Miettinen, T.A. (1999). Serum squalene in postmenopausal women without and with coronary artery disease. Atherosclerosis *146*, 61–64.

Raskin, P., and Siperstein, M.D. (1974). Mevalonate metabolism by renal tissue in vitro. J. Lipid Res. *15*, 20–25.

Rawson, R.B., DeBose-Boyd, R., Goldstein, J.L., and Brown, M.S. (1999). Failure to cleave sterol regulatory element-binding proteins (SREBPs) causes cholesterol auxotrophy in Chinese hamster ovary cells with genetic absence of SREBP cleavage-activating protein. J. Biol. Chem. *274*, 28549–28556.

Rodwell, V.W., Nordstrom, J.L., and Mitschelen, J.J. (1976). Regulation of HMG-CoA reductase. Adv. Lipid Res. *14*, 1–74.

Sakakibara, J., Watanabe, R., Kanai, Y., and Ono, T. (1995). Molecular cloning and expression of rat squalene epoxidase. J. Biol. Chem. *270*, 17–20.

Sever, N., Song, B.L., Yabe, D., Goldstein, J.L., Brown, M.S., and DeBose-Boyd, R.A. (2003). Insig-dependent ubiquitination and degradation of mammalian 3-hydroxy-3-methylglutaryl-CoA reductase stimulated by sterols and geranylgeraniol. J. Biol. Chem. *278*, 52479–52490.

Sharipo, A., Imreh, M., Leonchiks, A., Imreh, S., and Masucci, M.G. (1998). A minimal glycine-alanine repeat prevents the interaction of ubiquitinated I kappaB alpha with the proteasome: a new mechanism for selective inhibition of proteolysis. Nat. Med. *4*, 939–944.

Song, B.L., and DeBose-Boyd, R.A. (2004). Ubiquitination of 3-hydroxy-3-methylglutaryl-CoA reductase in permeabilized cells mediated by cytosolic E1 and a putative membrane-bound ubiquitin ligase. J. Biol. Chem. *279*, 28798–28806.

Song, B.L., Javitt, N.B., and DeBose-Boyd, R.A. (2005). Insig-mediated degradation of HMG CoA reductase stimulated by lanosterol, an intermediate in the synthesis of cholesterol. Cell Metab. *1*, 179–189.

Thomas, S., and Fell, D.A. (1998). The role of multiple enzyme activation in metabolic flux control. Adv. Enzyme Regul. *38*, 65–85.

Wong, J., Quinn, C.M., Gelissen, I.C., and Brown, A.J. (2008). Endogenous 24 (S),25-epoxycholesterol fine-tunes acute control of cellular cholesterol homeostasis. J. Biol. Chem. *283*, 700–707.

Yabe, D., Xia, Z.P., Adams, C.M., and Rawson, R.B. (2002). Three mutations in sterol-sensing domain of SCAP block interaction with insig and render SREBP cleavage insensitive to sterols. Proc. Natl. Acad. Sci. USA *99*, 16672–16677.

Yamamoto, S., and Bloch, K. (1970). Studies on squalene epoxidase of rat liver. J. Biol. Chem. *245*, 1670–1674.

Yang, J., Sato, R., Goldstein, J.L., and Brown, M.S. (1994). Sterol-resistant transcription in CHO cells caused by gene rearrangement that truncates SREBP-2. Genes Dev. *8*, 1910–1919.

Yang, T., Espenshade, P.J., Wright, M.E., Yabe, D., Gong, Y., Aebersold, R., Goldstein, J.L., and Brown, M.S. (2002). Crucial step in cholesterol homeostasis: sterols promote binding of SCAP to INSIG-1, a membrane protein that facilitates retention of SREBPs in ER. Cell *110*, 489–500.

Yang, C., McDonald, J.G., Patel, A., Zhang, Y., Umetani, M., Xu, F., Westover, E.J., Covey, D.F., Mangelsdorf, D.J., Cohen, J.C., and Hobbs, H.H. (2006). Sterol intermediates from cholesterol biosynthetic pathway as liver X receptor ligands. J. Biol. Chem. *281*, 27816–27826.